Mode-zero Robinson instability in the presence of passive superconducting harmonic cavities

Tianlong He,* Weiwei Li,† Zhenghe Bai, and Weimin Li

National Synchrotron Radiation Laboratory, University of Science and Technology of China, Hefei, Anhui, 230029, China

(Received 17 March 2023; accepted 12 June 2023; published 28 June 2023)

A higher harmonic cavity (HHC) is popularly employed in synchrotron light storage rings to enhance the machine performance, which requires its fundamental mode resonant frequency to be tuned above the radio-frequency harmonic. However, this detuning is likely to cause Robinson instability. In this paper, we focus on a mode-zero Robinson instability driven by the fundamental mode of a passive superconducting harmonic cavity (PSHC). This instability oscillates slightly below the detuning frequency of PSHC and was recently observed in tracking simulations or experiments for several synchrotron light sources, but the underlying mechanisms have not been well understood. To investigate this instability, we modify the conventional Robinson instability equation with the inclusion of the damping effect. By solving directly this modified equation combined with performing macroparticle tracking simulation, it is found that this instability is largely dependent on the momentum compaction factor, the Q value and detuning of PSHC, and even the radiation damping time. Most importantly, this instability can be significantly enhanced by a higher Q of PSHC and a lower radiation damping time, which is completely contrary to the conventional Robinson instability.

DOI: 10.1103/PhysRevAccelBeams.26.064403

I. INTRODUCTION

In synchrotron light storage rings, the higher harmonic cavity (HHC) is an essential component to attain the machine performance. By operating the HHC in the bunch lengthening mode, it can mitigate the intrabeam scattering induced emittance growth, increase the Touschek lifetime, and reduce the beam-induced heating of critical vacuum components. In addition, the HHC can also provide Landau damping by flattening the potential well to suppress the coupled bunch instability driven by higher-order modes in cavities [1,2]. However, the operation of HHC in bunch lengthening mode requires its fundamental mode resonant frequency has to be tuned higher than the radio-frequency (rf) harmonic. According to Robinson instability theory [3], it is known that this detuning is likely to cause beam instability, which may pose a limitation on the maximum bunch lengthening.

The instabilities related to the HHC fundamental mode and well understood mainly include the coupled dipole-quadrupole instability [4], typical mode-zero instability [5], and periodic transient beam-loading (PTBL) instability [6,7] (also known as the mode-1 instability [8]). The specific type of instability primarily depends on the relevant parameters, especially the parameters of HHC. In general, lowering the R/Q of HHC is beneficial to improve the current threshold of Robinson instability and mitigate the transient beam-loading effect introduced by uneven beam filling [9]. In this respect, the superconducting HHC has the advantage of considerably low R/Q and high Q, which is essential to alleviate such Robinson instabilities and beam-loading transients. So far, it has been installed in several third-generation storage rings and successfully operated in passive mode [10–12]. The passive superconducting harmonic cavity (PSHC) is also adopted by several fourth-generation storage rings [13–15]. Therefore, the instabilities related to PSHC will be focused on in this paper.

For PSHC, in addition to the aforementioned PTBL instability, which may limit the bunch lengthening at relatively high beam current, we also need to attach importance to another new Robinson instability, which is a mode-zero instability that oscillates slightly below the detuning frequency of PSHC and may lead to a lower current threshold to achieve optimum or near-optimum bunch lengthening. This new instability actually has already appeared in tracking simulations for several synchrotron light sources, such as ESRF-EBS [16], SLS [17],

*htlong@ustc.edu.cn
†liwe@ustc.edu.cn

and SOLEIL-II [18], and also in an experiment [17]. However, its mechanism has not been well understood. Since the PSHC is adopted by several storage rings, it is necessary to further explore the mechanism of this instability. In this paper, we modify the conventional Robinson instability equation by including the damping effect so that it can be well used to study this instability. By solving this equation, we find two solutions corresponding to two unstable modes. One of the modes corresponds exactly to this instability, which is found to be enhanced by a higher Q of PSHC and strong external damping. We perform a comprehensive study of its characteristics, which can help us find measures to suppress this instability.

This paper is organized as follows: In Sec. II, we introduce the formulas and the tracking method for the mode-zero Robinson instability. Both methods predict an unstable mode that has a frequency slightly lower than the detuning of PSHC and their results are in good agreement. In Sec. III, using the planned Hefei Advanced Light Facility (HALF) storage ring as an example, the dependence of the instability on relevant parameters is studied in detail, and the possible mode coupling and the influence of the main cavity fundamental mode are analyzed. Section IV discusses the instability of both SLS and SSRF storage rings. The conclusions and discussions are presented in Sec. V.

II. METHOD AND VERIFICATION

A. Mode-zero Robinson instability formulas

Following the typical derivations in Ref. [5] for the Robinson instability, the electron bunches circulating in the ring are modeled as pointlike rigid bunches, uniformly filled in rf buckets. Its longitudinal displacement can be written in the form of $z \propto e^{-i\Omega t}$, where Ω is the complex mode angular frequency of the beam oscillation. The real part $\mathrm{Re}[\Omega]$ gives the synchrotron frequency measured in a real operation, and the imaginary part $\mathrm{Im}[\Omega]$ gives the Robinson instability growth rate if $\mathrm{Im}[\Omega] > 0$ (or damping rate if $\mathrm{Im}[\Omega] < 0$). Then the Robinson instability driven by an arbitrary longitudinal impedance $Z_{||}$ can be described by

$$\Omega^2 - \omega_s^2 = -i\frac{\omega_0 I_0 \alpha_c}{2\pi E/e}\sum_{i=-\infty}^{\infty}[p\omega_0 Z_{||}(p\omega_0) - (p\omega_0+\Omega)Z_{||}(p\omega_0+\Omega)], \quad (1)$$

where ω_0 is the revolution angular frequency, I_0 is the average beam current, α_c is the momentum compaction factor, E is the beam energy, e is the electronic charge. $\omega_s = \sqrt{eV_{rf}h\omega_0\alpha_c \sin\varphi_s/(ET_0)}$ is the unperturbed synchrotron angular frequency, T_0 is the revolution period, h is the harmonic number, V_{rf} is the main cavity voltage assumed to be constant, φ_s is the corresponding synchronous phase, determined by $V_{\mathrm{rf}}\sin\varphi_s = U_0$, with U_0 being the energy loss per turn.

Note that the external damping effect is not considered in the above equation. When it is considered, Eq. (1) should be modified as

$$\Omega^2 + i\frac{2\Omega}{\tau_z} - \omega_s^2 = -i\frac{\omega_0 I_0 \alpha_c}{2\pi E/e}\sum_{i=-\infty}^{\infty}[p\omega_0 Z_{||}(p\omega_0) - (p\omega_0+\Omega)Z_{||}(p\omega_0+\Omega)], \quad (2)$$

where τ_z is the damping time from radiation damping or other damping mechanisms. The corresponding damping rate is given as $1/\tau_z$.

Regarding the impedance contributor for the right-hand side of Eq. (2), for simplicity, we will only consider the PSHC fundamental mode. In other words, we will assume an ideal sine wave for the main rf cavity, ignoring the influence of its fundamental mode on beam dynamics such as the synchrotron frequency shift [19] and the Robinson damping rate. As for PSHC, its fundamental mode can be expressed by

$$Z_{||}(\omega) = \frac{R}{1 + iQ(\frac{\omega_r}{\omega} - \frac{\omega}{\omega_r})}, \quad (3)$$

where Q is the quality factor, R is the shunt impedance, and $\omega_r = nh\omega_0 + 2\pi\Delta f_r$ is the resonant angular frequency, where n is the harmonic order of PSHC, and Δf_r is the detuning frequency of PSHC.

For the mode-zero Robinson instability, the only significant contributions on the right-hand side of Eq. (2) come from terms $p = \pm nh$ in the summation, because ω_r is very close to $nh\omega_0$. This gives

$$\Omega^2 + i\frac{2\Omega}{\tau_z} - \omega_s^2 = -i\frac{\omega_0 I_0 \alpha_c}{2\pi E/e}\{i2nh\omega_0 \mathrm{Im}[Z_{||}(nh\omega_0)] - \omega_p^+ Z_{||}(\omega_p^+) - \omega_p^- Z_{||}(\omega_p^-)\}, \quad (4)$$

where $\omega_p^{\pm} = \pm nh\omega_0 + \Omega$. Since the deviation $\Delta f_r/f_r$ is normally small, we have

$$\mathrm{Im}[Z_{||}(nh\omega_0)] \approx -\frac{Rf_r}{2Q\Delta f_r}. \quad (5)$$

Substitute Eq. (5) into Eq. (4), then we finally obtain

$$\Omega^2 + i\frac{2\Omega}{\tau_z} - \omega_s^2 + i\frac{\omega_0 I_0 \alpha_c}{2\pi E/e} \times \left\{-i\frac{nh\omega_0 R f_r}{Q\Delta f_r} - \omega_p^+ Z_{||}(\omega_p^+) - \omega_p^- Z_{||}(\omega_p^-)\right\} = 0. \quad (6)$$

The above equation can in principle be solved to obtain Ω. Some authors introduce the assumption that Ω does not deviate much from ω_s for the modest beam intensities so that Ω can be solved analytically [5]. However, in doing so, one will miss another unstable solution related to the

detuning frequency for the case of PSHC. So it is better to solve Eq. (6) numerically without approximation.

It is known that Ω is a complex number, so it can be expressed by $\Omega_r + i\Omega_i$. We need to find the specific $(\Omega_{r0}, \Omega_{i0})$ to satisfy Eq. (6), that is, to make that $g(\Omega_{r0} + i\Omega_{i0}) = 0$, where we define

$$g(\Omega) = \Omega^2 + i\frac{2\Omega}{\tau_z} - \omega_s^2 + i\frac{\omega_0 I_0 \alpha_c}{2\pi E/e} \times \left\{ -i\frac{nh\omega_0 R f_r}{Q\Delta f_r} - \omega_p^+ Z_{||}(\omega_p^+) - \omega_p^- Z_{||}(\omega_p^-) \right\}. \quad (7)$$

We can scan the complex angular frequency in a certain range to find the roots. Ω_r is in the range from 0 to $\Delta\omega_r$, and Ω_i should be in a wide enough range, such as -2000 to 2000 1/s. That is, $(\Omega_{r0}, \Omega_{i0})$ is limited in a rectangular two-dimensional (2D) domain. A direct idea is to discretize this 2D domain with a suitable mesh size and then calculate the value of $g(\Omega)$ for all discrete points, where the minimum of $|g(\Omega)|$ corresponds to the required $\Omega_{r0} + i\Omega_{i0}$. It will be shown later that for the PSHC case, $|g(\Omega)|$ generally has two local minima, one's real part close to the synchrotron frequency and another close to the detuning frequency. To facilitate the subsequent discussion, the former is labeled as S mode and the latter as D mode. It should be mentioned that a similar analysis but for the main cavity accelerating mode was done by Towne and Wang [20]. They obtained an equation similar to Eq. (6). Two modes of oscillation were also derived, named separately beam mode and cavity mode, which correspond to the S mode and D mode here, respectively. The D-mode oscillation is exactly related to the mode-zero Robinson instability and is focused on in this paper.

B. Macroparticle tracking

The STABLE code will be used to conduct the tracking simulations for the mode-zero Robinson instability study. This code is implemented in a MATLAB environment with the usage of the state-of-the-art of graphics-processing-unit acceleration technique so that the tracking efficiency is significantly improved, and the postprocessing of tracking results can be very convenient. It can be used to study longitudinal beam dynamics considering arbitrary fill patterns, passive harmonic cavities, higher order modes, and arbitrary short-range wake. More details about the STABLE are given in Ref. [21]. For the case of PSHC, to be consistent with Eq. (6), which is derived based on pointlike rigid bunch model and includes only the effects of damping and the fundamental mode of PSHC, we perform the STABLE tracking with a single macroparticle per bunch and ignoring the main cavity beam loading. While, when it comes to analyzing the influence of the main cavity beam loading in Sec. III F, each bunch is modeled as 10,000 macroparticles and the quantum excitation is included automatically. At the beginning of tracking, the voltage phasor of PSHC should be initialized and can be determined by the following formula:

$$\tilde{V}_{hc} = I_0 \frac{R}{Q}\frac{f_r}{\Delta f_r}\exp(i\varphi_{hc}), \quad (8)$$

where φ_{hc} is the detuning phase and related to the detuning frequency by $\varphi_{hc} = \arctan(\frac{2Q\Delta f_r}{f_r})$.

C. Verification of Eq. (6)

To verify Eq. (6), the HALF storage ring that will install a one-cell PSHC for bunch lengthening is taken as the research object. The main parameters of the HALF storage ring with insertion devices are summarized in Table I. To create conditions for mode-zero instability, the average current is set to 40 mA and the assumed filling pattern is eight equally spaced and charged bunches. At this current, the corresponding near-optimum detuning of PSHC is about 6 kHz. The radiation damping time is $\tau_z = 14$ ms. For comparison, we also study the case of $\tau_z = 2$ ms, and additional damping could be provided by a bunch-by-bunch feedback system. In the calculation of Eq. (7), we typically take the scan range of $\Omega_r \in [0, \Delta\omega_r]$ and $\Omega_i \in [-2000, 2000]$ 1/s with step size $\Delta\Omega_r = 4\pi$ Hz rad and $\Delta\Omega_i = 2$ 1/s.

The contour map of the logarithm of $|g(\Omega)|$ for the cases of $\tau_z = 2$ ms and $\tau_z = 14$ ms is shown in Fig. 1. We can see that there are two local minima, as mentioned earlier, the left one is related to the S-mode solution and the other D-mode solution. The imaginary part of S-mode one is negative, and its value is approximately equal to the external damping rate; while the imaginary part of D-mode one is 18 1/s for $\tau_z = 2$ ms, and -20 1/s for $\tau_z = 14$ ms. It indicates that, interestingly, the beam becomes unstable with a stronger damping rate, which is completely contrary to any other typical collective beam instability.

TABLE I. Main parameters of the HALF storage ring used for mode-zero Robinson instability study.

Parameter	Symbol	Value
Beam energy	E	2.2 GeV
Ring circumference	C	479.86 m
Assumed beam current	I_0	40 mA
Longitudinal damping time	τ_z	14 ms
Momentum compaction	α_c	9.4×10^{-5}
Harmonic number	h	800
Energy loss per turn	U_0	400 keV
Main cavity voltage	V_{rf}	1.2 MV
HHC harmonic order	n	3
HHC normalized shunt impedance	R/Q	39 Ω
HHC quality factor	Q	2×10^8
HHC near-optimum detuning	Δf_r	6 kHz

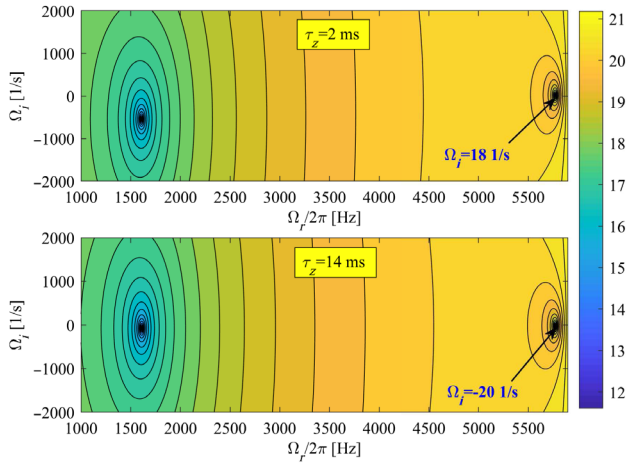

FIG. 1. The contour map of $\log(|g(\Omega)|)$ for the cases of damping time $\tau_z = 2$ ms (top) and $\tau_z = 14$ ms (bottom). The longitudinal coordinate represents the growth rate (if $\Omega_i > 0$) or damping rate (if $\Omega_i < 0$).

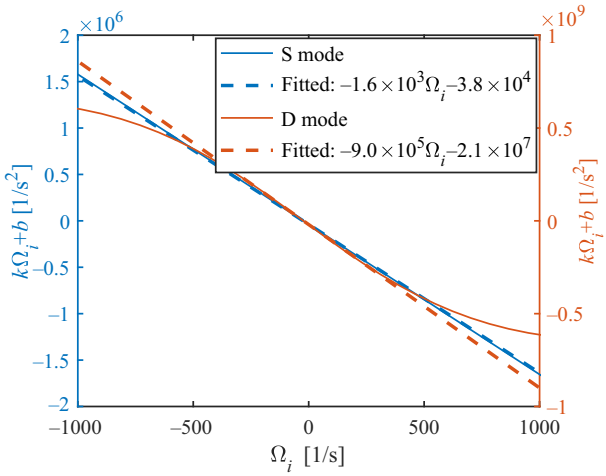

FIG. 2. Linear fitting of Eq. (10) for both S and D modes. The solid data are obtained by calculating the left part of Eq. (10), and the dashed data by linear fitting of the solid data. For both S and D modes, the linear fitting is accurate in an appropriate range.

To check the semianalytical calculation, the STABLE code is used to conduct tracking simulations for the above cases. Each bunch is modeled as a single macroparticle, and 50,000 turns are tracked. The growth or damping rate can be obtained by fitting the oscillation of averaged relative momentum deviation in its exponential rising or falling stage. The tracking results are 17.9 and −19.5 1/s for $\tau_z = 2$ ms and $\tau_z = 14$ ms, respectively, which are in good agreement with the semianalytical results. More verification of Eq. (6) can be found in Sec. III.

D. Analysis of the D-mode instability

Let us further analyze it mathematically. The root $(\Omega_{r0}, \Omega_{i0})$ of Eq. (6) needs to satisfy that both the real and imaginary parts of function $g(\Omega_{r0} + i\Omega_{i0})$ become zero. Assume that Ω_{r0} is already known but Ω_{i0} unknown, then one can obtain

$$\mathrm{Im}[g(\Omega_{r0} + i\Omega_i)] = 2\Omega_{r0}\Omega_i + \frac{2\Omega_{r0}}{\tau_z} + \frac{\omega_0 I_0 \alpha_c}{2\pi E/e} \times \mathrm{Re}\{-\omega_p^+ Z_{||}(\omega_p^+) - \omega_p^- Z_{||}(\omega_p^-)\} = 0. \tag{9}$$

For a certain Ω_{r0}, it is found that the third term on the right-hand side of Eq. (9) is approximately linearly dependent on Ω_i in an appropriate range as shown in Fig. 2, then we have

$$\frac{\omega_0 I_0 \alpha_c}{2\pi E/e}\mathrm{Re}\{-\omega_p^+ Z_{||}(\omega_p^+) - \omega_p^- Z_{||}(\omega_p^-)\} \approx k\Omega_i + b, \tag{10}$$

where k and b are real coefficients that depend on Ω_{r0} and can be obtained by data fitting. Substitute Eq. (10) into Eq. (9), then we have

$$\Omega_{i0} = -\frac{b + \frac{2\Omega_{r0}}{\tau_z}}{2\Omega_{r0} + k}. \tag{11}$$

Still using the parameters listed in Table I for the case of 2 ms, the value of the left-hand side of Eq. (10) and the fitting curves $k\Omega_i + b$ as a function of Ω_i for both S and D modes are shown in Fig. 2, and the values of each item in Eq. (11) are summarized in Table II. As seen in Fig. 2, the left-hand side of Eq. (10) for S mode has a relative large linear regime over $\Omega_i \in [-1000, 1000]$, while that of D mode has a smaller linear regime $\Omega_i \in [-300, 300]$, but the growth rate of D mode is only about 18 1/s as mentioned in Sec. II C and still located in the linear regime.

For the S mode, the denominator on the right-hand side of Eq. (11) is $2\Omega_{r0} + k \approx 2\Omega_{r0}$, and the numerator is $b + 2\Omega_{r0}/\tau_z \approx 2\Omega_{r0}/\tau_z$, so it indicates that the damping rate of S mode is dominated by radiation damping. It should be noted that the approximation made here is only valid for the parameters that have been chosen. Of course,

TABLE II. Values of each item in Eq. (11) for both S and D mode.

Mode	$\Omega_{r0}/2\pi$ [1/s]	$2\Omega_{r0}/\tau_z$ [1/s²]	b [1/s²]	$2\Omega_{r0}$ [1/s]	k [1/s]	Ω_{i0} [1/s]
S	1609	1.0×10^7	-3.8×10^4	2.0×10^4	-1.6×10^3	−541
D	5773	3.6×10^7	-2.1×10^7	7.3×10^4	-9.0×10^5	18.1

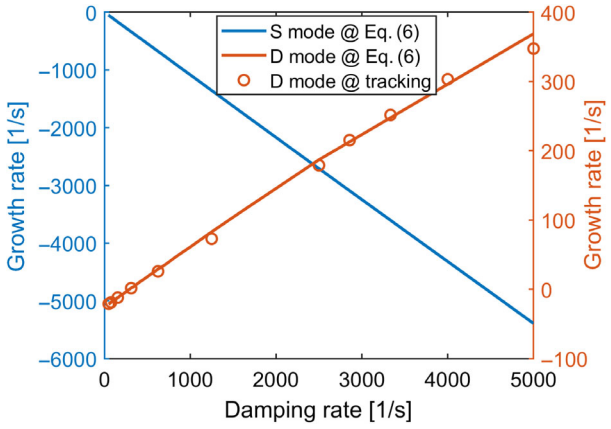

FIG. 3. Growth rate of the mode-zero Robinson instability as a function of the damping rate (1/damping time).

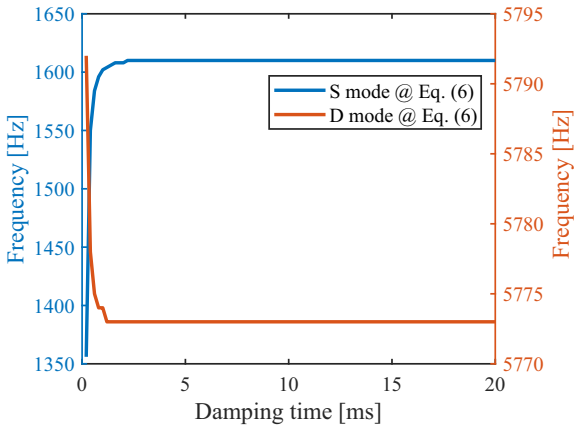

FIG. 4. Oscillation frequency as a function of damping time, obtained by solving Eq. (6).

for other parameters, the Robinson (S mode) growth rate may not be dominated by the radiation damping. In addition, the value of k is negative, and it implies that the radiation damping plays a role in the energy exchange between the beam and rf field in the PSHC and enhances the total damping of S mode further. For the D mode, the denominator of $2\Omega_{r0} + k$ is even less than zero as seen in Table II, and it indicates that the radiation damping, on the contrary, will contribute to the total growth rate of D mode.

III. DEPENDENCE OF THE MODE-ZERO ROBINSON INSTABILITY

We have shown that the D-mode oscillation growth is enhanced with a shorter damping time in the presence of PSHC. For storage rings employing PSHC, it is of practical significance to explore how to avoid this atypical Robinson instability. In this section, we will investigate the dependence of the Robinson instability on relevant parameters, including damping time, Q value and detuning of PSHC, and momentum compaction factor. Moreover, the possible mode coupling and the impact of the main cavity fundamental mode are also investigated.

A. Damping time

We first study the effect of the damping time with the parameters listed in Table I. The cases with two different damping times have been displayed in Sec. II C. To explore more cases, the damping time is varied from 0.2 to 20 ms with a step of 0.2 ms, and the growth rates obtained from Eq. (6) and tracking are illustrated in Fig. 3. It should be pointed out that the instability growth rates (or damping rates) given by tracking are dominated by the least stable mode, so the tracking method here can only provide the D-mode growth rates. It can be seen that the S-mode growth rates are dominated by the damping rate $-1/\tau_z$ and always less than zero, while the D-mode growth rates show the approximate inverse dependence on the damping time, and beam stability requires $\tau_z > 3.4$ ms. That is consistent with the analysis in Sec. II D. Thus, for HALF with a damping time of 14 ms, the mode-zero Robinson instability can be avoided.

Figure 4 shows the oscillation frequency as a function of damping time for both S and D modes. The damping time is also scanned in the range from 0.2 to 20 ms with a step of 0.2 ms. We can see that the damping affects hardly the frequency of both modes. Only when less than 1 ms, reducing the damping time increases and decreases the D-mode and S-mode frequencies, respectively.

B. PSHC quality factor

In our previous study of bunch lengthening for the HALF storage ring, we have shown that a smaller R/Q of HHC is conducive to obtaining a longer bunch lengthening without PTBL at a higher beam current [6]. This impelled HALF to adopt one-cell PSHC with R/Q less than 40 Ω. For PSHC around 1.5 GHz, a typical unloaded Q factor is of order 10^8, but combined with a power coupler, the loaded quality factor can be adjusted to about 2×10^5, such as the PSHC of APS Upgrade storage ring [13]. Thus, we vary the Q value from 2×10^5 to 10^9 while keeping the detuning constant and assume the HALF storage ring has a damping time of 2 ms. For these cases, the corresponding growth rates obtained by both solving Eq. (6) and tracking simulation are shown in Fig. 5. A smaller Q helps suppress the D-mode instability but may enhance the S-mode instability. So a moderate Q of order 10^6–10^7 is better suited to damp both S- and D-mode instabilities.

We note that the D-mode oscillation will be strongly damped when the Q value is lower than 10^7, which is why the D-mode instability only occurs in the case of a high Q of PSHC. For the case of low Q, such as PSHC with a coupler to extract beam power, the D-mode instability is not expected to occur.

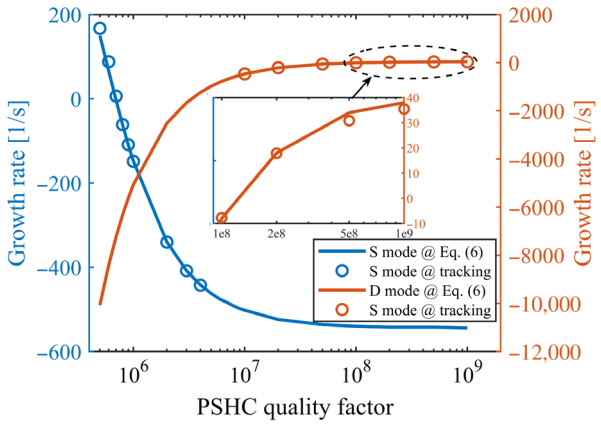

FIG. 5. Growth rate of mode-zero Robinson instability as a function of PSHC quality factors.

C. PSHC detuning

Figure 6 shows the D-mode growth rates as a function of PSHC detuning for the case of HALF with damping times of 2 and 14 ms. The D-mode growth rate increases as the detuning decreases. For the case of $\tau_z = 14$ ms, the D mode is always damped in the detuning range from 5 to 12 kHz, indicating that it can be avoided by HALF in reality. While, for the case of $\tau_z = 2$ ms, there is a threshold detuning, below which the D-mode oscillation will exponentially grow and eventually lead to beam loss. Therefore, when it is necessary to lower the detuning to obtain the required bunch lengthening at a relatively low beam current, the D-mode instability may be excited, especially for those rings with relatively small damping time.

D. Momentum compaction factor

Since the momentum compaction factor plays an important role in longitudinal beam dynamics, it is necessary, in detail, to study its impact on the mode-zero Robinson instability in the case of PSHC. Still using the parameters listed in Table I but only changing the momentum compaction factor from α_{c0} to $4\alpha_{c0}$ with α_{c0} being 9.4×10^{-5}, the complex angular frequencies obtained by solving Eq. (6) are shown in Fig. 7. For both damping times, as momentum compaction factor increases, the oscillation frequencies of S and D modes are increased and decreased respectively, while, the growth rates of S and D modes are decreased and increased, respectively. Therefore, the larger the momentum compaction factor, the more unstable the D-mode oscillation.

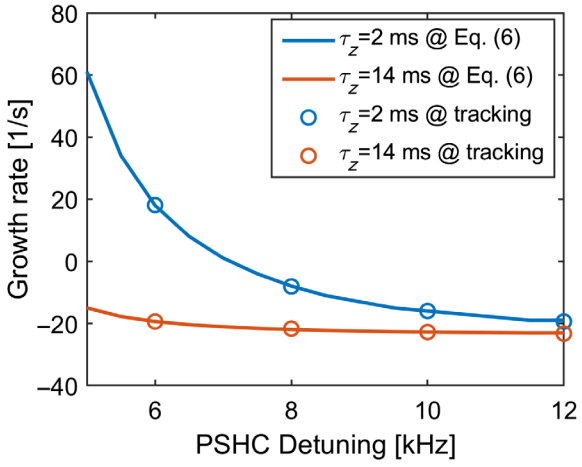

FIG. 6. Growth rate of the D-mode Robinson instability as a function of PSHC detuning.

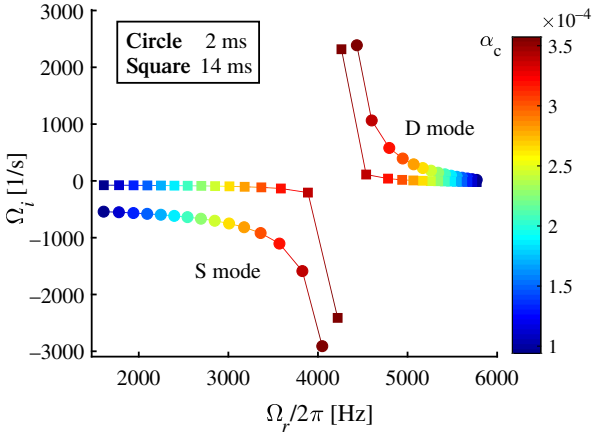

FIG. 7. Complex angular frequencies as a function of momentum compaction factor for the cases of $\tau_z = 2$ and 14 ms.

For the storage ring with a large momentum compaction factor and the requirement to achieve sufficient bunch lengthening at a relatively low beam current, the coupling of the S and D modes is likely to occur. Because the S-mode frequency is relatively high, and on the other hand, the PSHC detuning has to be low to obtain the desired voltage, thus lowering the D-mode frequency. Both factors create conditions for mode coupling. In the next subsection, we will further discuss the case of mode coupling.

E. Coupling of S and D modes

It is noteworthy that this coupling of S and D modes was also observed in the simulation for SOLEIL-II [22], in which the detuning was reduced to close to the synchrotron frequency, thus creating conditions for the mode coupling. However, this mode coupling was yet fully understood. In this subsection, we take HALF parameters as an example to study it further via solving Eq. (6). To create conditions for the mode coupling, the momentum compaction factor is magnified by a factor of 4.

Figure 8 shows the complex angular frequency as a function of PSHC detuning in the range from 4 to 7 kHz. For the cases of both damping times of 2 and 14 ms, it can be seen that as the detuning decreases, the two modes finally merge at a detuning of about 6200 Hz. After that, the complex frequency values of S and D modes are

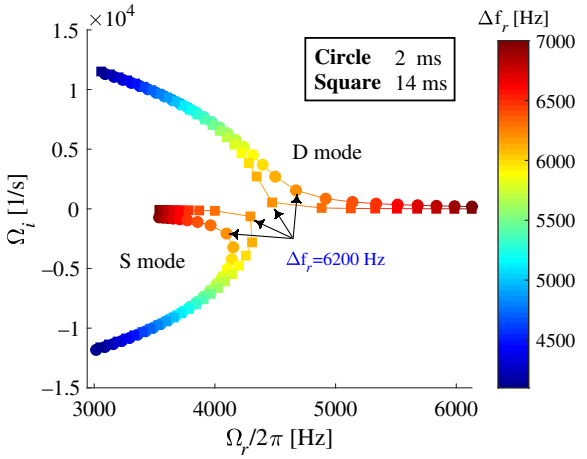

FIG. 8. Complex angular frequencies as a function of PSHC detuning for the cases of $\tau_z = 2$ and 14 ms.

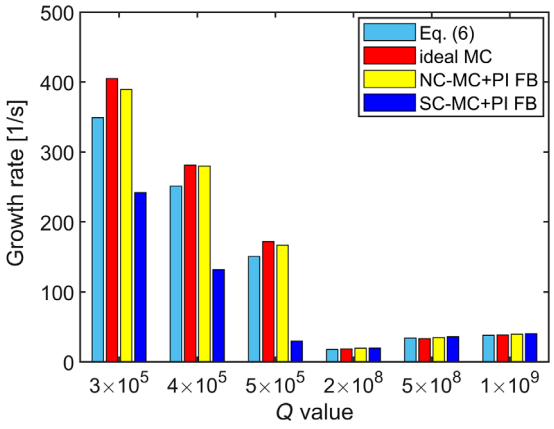

FIG. 9. The mode-zero Robinson instability growth rates as a function of the PSHC quality factor. The S-mode instability corresponds to the cases of $Q = 3 \times 10^5$, 4×10^5, and 5×10^5, and the D-mode instability corresponds to the cases of $Q = 2 \times 10^8$, 5×10^8, and 1×10^9. The legend gives the calculation consideration: "ideal MC" means ignoring the main cavity fundamental mode effect; "NC-MC + PI FB" and "SC-MC + PI FB" mean, respectively, the normal-conducting and the superconducting main cavity with turning on the PI feedback controller.

approximately conjugate with each other, which is strong evidence for the mode coupling. It should be noted that after the mode coupling occurs, the D-mode growth rate will be very large and not be easily calculated accurately by tracking simulation because of the beam being lost in a few tracking turns. Solving Eq. (6) provides us with a convenient and accurate method to study the mode coupling effect.

This kind of mode coupling phenomenon is unlikely to appear in the new generation of storage rings because of the generally suppressed horizontal dispersion that reduces the momentum compaction factor and the synchrotron frequency unless the detuning of PSHC is very low to achieve the required bunch lengthening at low beam current.

F. Main cavity fundamental mode

The influence of the main cavity fundamental mode on the mode-zero Robinson instability, which was not covered in the previous analysis, will be analyzed by using macroparticle tracking in this subsection. As shown in Fig. 5, with an external damping time of 2 ms, the S mode and D mode will become unstable when $Q \leq 6 \times 10^5$ and $Q \geq 2 \times 10^8$, respectively. These cases can be chosen as good examples to investigate the influence of the main cavity fundamental mode on the mode-zero Robinson instability. For the HALF storage ring, we consider two schemes of main cavity: two normal-conducting (NC) rf cavities with total $R/Q = 160\ \Omega$, loaded $Q = 2 \times 10^4$ and detuning frequency -6 kHz; and one-cell superconducting (SC) rf cavity with $R/Q = 45\ \Omega$, loaded $Q = 2 \times 10^5$ and detuning frequency -1 kHz. The detuning frequencies given above are to make the loaded angle (the angle between the cavity voltage phasor and the generator current phasor) approximately -10 deg at 40 mA.

The STABLE code is used to perform tracking simulations with 10,000 macroparticles per bunch. The newly implemented proportional-integral feedback (PI FB) control module in the STABLE code can be used to model the low-level rf control system more realistically, aiming at keeping constant the cavity voltage phasor. The PI FB module will be turned on when considering the main cavity fundamental mode. For the two types of main cavities, complete simulations including the quantum excitation are performed. As a comparison, the case of the ideal main cavity is also computed. The instability growth rates as a function of the PSHC Q values obtained from tracking simulations for the above three cases and from Eq. (6) for the case without the main cavity fundamental mode effect are shown in Fig. 9.

It can be seen that the D-mode growth rates are almost unaffected by the main cavity fundamental mode, no matter for the NC or SC main cavity. For the S-mode growth rates, there are clear discrepancies between the cases of SC and NC: The S-mode growth rates are effectively reduced with the inclusion of the SC main cavity; while they are almost unchanged for the NC main cavity. That is to say, the main cavity fundamental mode can reduce the S-mode growth rate contributed by the PSHC, but the degree of reduction largely depends on the specific parameters of the main cavity.

IV. APPLICATION TO SLS AND SSRF STORAGE RINGS

For the HALF storage ring, we have studied the characteristics of mode-zero Robinson instability driven by the fundamental mode of PSHC by artificially changing its relevant parameters. Due to its relatively long damping

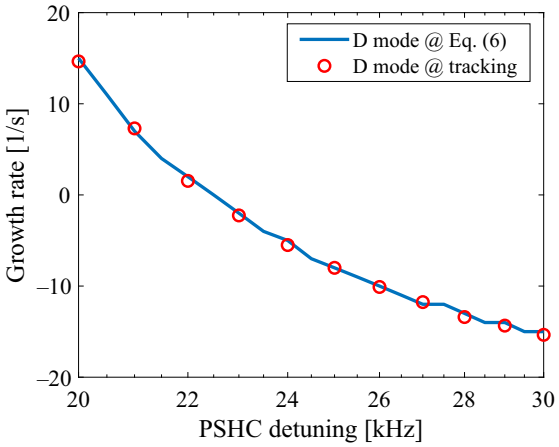

FIG. 10. D-mode growth rate as a function of PSHC detuning for the case of SLS with 100 mA beam current and 40 equally spaced bunches.

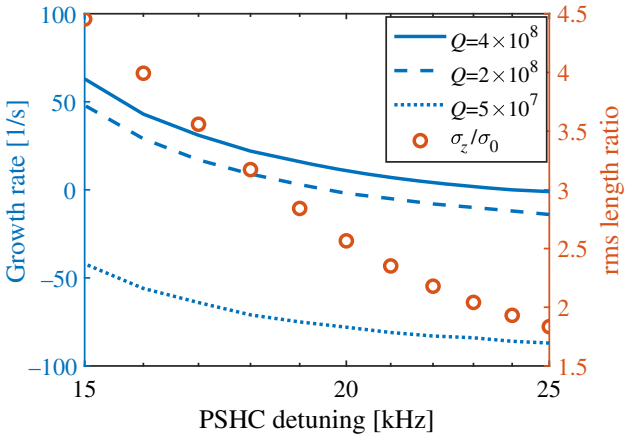

FIG. 11. D-mode growth rate and bunch lengthening ratio as a function of PSHC detuning. The growth rates are obtained by solving Eq. (6) for SSRF at 200 mA. The legend in the blue line gives the quality factor of PSHC. The legend of σ_z/σ_0 is the ratio of the rms bunch length to the natural length, and it is obtained using a semianalytical method [25] without considering the main cavity beam loading.

time of 14 ms, the D-mode instability can be avoided at near-optimum detuning and beam current of 40 mA. When reducing the damping time to 2 ms, the conditions of the D-mode instability are created artificially, so its characteristics can be studied. In addition to the damping time, we have known that in the case of a relatively large momentum compaction factor, low detuning, and high Q of PSHC, the D-mode instability is more likely to occur.

Now, let us turn our attention to some existing synchrotron light sources that have already run PSHC, including SLS [10], ELETTRA [11], and SSRF [12]. According to their parameters, we take SLS and SSRF as examples, since they have a relatively short damping time and a relatively large momentum compaction factor and thus are more likely to encounter such D-mode instability. In fact, for the case of SLS with 100 mA beam current and 40 filled bunches, it was already reported that there is a threshold detuning of about 23.6 kHz [17], below which, both the bunch energy spread and the PSHC voltage start to oscillate, ultimately leading to beam loss. In Ref. [17], the threshold detuning for the beam loss was explained by Bosch's dipole-quadrupole coupling theory [4]. For this case, we study the D-mode instability using the same SLS parameters given in Ref. [17]. The growth rates as a function of detuning frequency obtained by solving Eq. (6) and tracking simulation are shown in Fig. 10. The threshold detuning is about 22.5 kHz, which is in good agreement with the aforementioned 23.6 kHz. It indicates that the beam loss observed in Ref. [17] can also be explained by the D-mode Robinson instability mechanism.

In particular, the PSHC of SSRF is made in pure niobium, which has a relatively large internal quality factor at an operating temperature [12]. Therefore, SSRF may encounter D-mode instability at a modest beam current. For the case of SSRF at 200 mA, we evaluate its D-mode growth rates and bunch lengthening ratio as a function of PSHC detuning. The new lattice parameters of SSRF used for this calculation are taken from [23]. The main cavity voltage and the PSHC R/Q are set to 4.5 MV and 88 Ω, respectively, according to Ref. [12]. In addition, the damping time is set to 3.5 ms [24]. The corresponding results are shown in Fig. 11. It can be seen that for the case of PSHC $Q = 2 \times 10^8$, SSRF is likely to encounter D-mode instability at a detuning of less than 20 kHz, which may limit the bunch lengthening ratio. To suppress the D-mode instability, the loaded quality factor of PSHC can be appropriately reduced, e.g., for the case of $Q = 5 \times 10^7$, PSHC can work even at a lower detuning of 15 kHz without the D-mode instability, allowing a larger bunch lengthening ratio.

V. CONCLUSIONS AND DISCUSSIONS

In this paper, by adding the damping effect to the conventional Robinson instability equation, we obtained a modified equation that can be used to analyze the mode-zero Robinson instability driven by the PSHC fundamental mode. By solving this equation, it was found that there are two oscillation modes related to mode-zero Robinson instability, one of which is related to the synchrotron frequency, called S-mode instability, and the other is related to the detuning of PSHC, called D-mode instability. For the D-mode instability, one of its major characteristics is that it is antidamped by radiation damping, which is contrary to the conventional Robinson instability. Another is that it can be mitigated by reducing the loaded quality factor of PSHC. In addition, the coupling of S and D modes can appear if the PSHC detuning is reduced further to approach the synchrotron frequency for the required PSHC voltage at a relatively low current. For the new generation of

synchrotron light sources, due to their relatively long damping time and small momentum compaction factor, the D-mode instability is suppressed to some extent, while the S-D mode coupling may limit the bunch lengthening ratio in the case of relatively low current.

It should be noted that we ignored the influence of the short-range wake on the S-D mode coupling. The short-range wake will lead to a synchrotron frequency shift, which will affect the coupling of S and D modes. As is observed by tracking simulation in Ref. [22], the short-range wake intensifies the mode coupling. Because Eq. (6) does not contain the short-range wake, it may lose accuracy for the mode coupling in the case of a strong short-range wake. We demonstrated the influence of the main cavity fundamental mode on the mode-zero Robinson instability driven by the PSHC using the HALF storage ring parameters. For the D-mode instability, the influence can be ignored. While, for the S-mode instability, the influence largely depends on the parameters of the main cavity fundamental mode. Further exploration and confirmation are needed to determine whether the above conclusions are applicable to other synchrotron light source ring parameters. To sum up, the PSHC fundamental mode can play a dominant role in the mode-zero Robinson instability, and solving Eq. (6) can provide convincing results for the D-mode instability.

ACKNOWLEDGMENTS

This research was supported by the National Natural Science Foundation of China (No. 12105284 and No. 11875259) and the Fundamental Research Funds for the Central Universities (No. WK2310000090).

[1] R. Nagaoka and K. L. F. Bane, Collective effects in a diffraction-limited storage ring, J. Synchrotron Radiat. **21**, 937 (2014).

[2] F. J. Cullinan, Å. Andersson, and P. F. Tavares, Harmonic-cavity stabilization of longitudinal coupled-bunch instabilities with a nonuniform fill, Phys. Rev. Accel. Beams **23**, 074402 (2020).

[3] K. W. Robinson, Stability of beam in radiofrequency system, Cambridge Electron Accelerator, MA, Technical Report No. CEAL-1010, 1964.

[4] R. A. Bosch, K. J. Kleman, and J. J. Bisognano, Robinson instabilities with a higher-harmonic cavity, Phys. Rev. ST Accel. Beams **4**, 074401 (2001).

[5] A. W. Chao, *Physics of Collective Beam Instabilities in High Energy Accelerators* (Wiley, New York, 1993), p. 162

[6] T. L. He, W. W. Li, Z. H. Bai, and L. Wang, Periodic transient beam loading effect with passive harmonic cavities in electron storage rings, Phys. Rev. Accel. Beams **25**, 024401 (2022).

[7] T. L. He, Novel perturbation method for judging the stability of the equilibrium solution in the presence of passive harmonic cavities, Phys. Rev. Accel. Beams **25**, 094402 (2022).

[8] M. Venturini, Passive higher-harmonic rf cavities with general settings and multibunch instabilities in electron storage rings, Phys. Rev. Accel. Beams **21**, 114404 (2018).

[9] J. M. Byrd, S. De Santis, J. Jacob, and V. Serriere, Transient beam loading effects in harmonic rf systems for light sources, Phys. Rev. ST Accel. Beams **5**, 092001 (2002).

[10] M. Pedrozzi, J. Raguin, W. Gloor, A. Anghel, M. Svandrlik, G. Penco, P. Craievich, A. Fabris, C. Pasotti, E. Chiaveri, R. Losito, S. Marque, O. Aberle, P. Marchand, P. Bosland, S. Chel, P. Brédy, and G. Devanz, SLS Operational Performance with Third Harmonic Superconducting System, in *Proceedings of the 11th Workshop on RF superconductivity, Lübeck/Travemünde, Germany* (JACoW, Lübeck, Germany, 2003), MOP25, pp. 91–94.

[11] G. Penco and M. Svandrlik, Experimental studies on transient beam loading effects in the presence of a superconducting third harmonic cavity, Phys. Rev. ST Accel. Beams **9**, 044401 (2006).

[12] Z. G. Zhang, Y. B. Zhao, K. Xu, X. Zheng, Q. Chang, S. J. Zhao, Z. Y. Ma, H. R. Jiang, W. F. Yang, X. F. Huang, Y. Wang, J. Shi, and H. T. Hou, Low level radio frequency controller for superconducting third harmonic cavity at SSRF, Nucl. Tech. **45**, 120101 (2022).

[13] M. P. Kelly, A. Barcikowski, J. Carwardine, Z. A. Conway, D. Horan, M. Kedzie, S. H. Kim, P. N. Ostroumov, J. Rathke, T. Schultheiss, and G. J. Waldschmidt, Superconducting harmonic cavity for the Advanced Photon Source Upgrade, in *Proceedings of the IPAC2015, Richmond, VA* (JACoW, Geneva, Switzerland, 2015), WEPTY008, pp. 3267–3269.

[14] I. C. Almeida, A. P. B. Lima, and M. H. Wallner, Third harmonic superconducting cavity for bunch lengthening and beam lifetime increase of Siruis synchrotron light source, in *Proceedings of the SRF2021, East Lansing, MI* (JACoW, Geneva, Switzerland, 2021), SUPCAV011, pp. 37–41.

[15] Y. Wei, J. Pang, B. Du, D. Jia, S. Zhang, and G. Feng, Design of a passive superconducting harmonic cavity for HALF storage ring, in *Proceedings of the 13th International Particle Accelerator Conference, IPAC2022, Bangkok, Thailand* (JACoW, Geneva, Switzerland, 2022), TUPOTK065, pp. 1378–1380.

[16] N. Carmignani, J. Jacob, B. Nash, and S. White, Harmonic RF system for the ESRF EBS, in *Proceedings of the IPAC2017, Copenhagen, Denmark* (JACoW, Geneva, Switzerland, 2021), THPAB003, pp. 3684–3687.

[17] L. Stingelin, Tracking simulations and tests results in SLS with Super-3HC, in *Proceedings of HarmonLIP 2022, Lund*, MAX IV (2022), https://indico.maxiv.lu.se/event/5098/contributions/6755/attachments/1171/2310/20221001HarmonLIPworkshopV2.pptx.

[18] A. Gamelin, Harmonic cavity studies for the SOLEIL Upgrade, in *Proceedings of iFAST Workshop 2022 Beam Diagnostics and Dynamics in Ultra-low Emittance Rings, Virtual Workshop* (2022), https://indico.scc.kit.edu/event/

2592/sessions/2579/attachments/5006/7591/Slides_3-1_Gamelin.pdf.

[19] N. Wang, Y. Zhang, C. H. Yu, G. Xu, and J. P. Dai, Synchrotron tune shift due to the fundamental mode of the RF cavities, Nucl. Instrum. Methods Phys. Res., Sect. A **1014**, 165725 (2021).

[20] N. Towne and J.-M. Wang, Spectrum of single bunch longitudinal dipole modes, Phys. Rev. E **57**, 3461 (1998).

[21] T. L. He and Z. H. Bai, Graphics-processing-unit-accelerated simulation for longitudinal beam dynamics of arbitrary bunch trains in electron storage rings, Phys. Rev. Accel. Beams **24**, 104401 (2021).

[22] A. Gamelin, SOLEIL II project review, in *Proceedings of HarmonLIP 2022, Lund, MAX IV* (2022), https://indico.maxiv.lu.se/event/5098/contributions/6752/attachments/1169/2312/HarmonLIP2022_SOLEIL.pptx.

[23] X. Wu, S. Q. Tian, X. Z. Liu, W. Z. Zhang, and Z. T. Zhao, Design and commissioning of the new SSRF storage ring lattice with asymmetric optics, Nucl. Instrum. Methods Phys. Res., Sect. A **1025**, 166098 (2022).

[24] B. C. Jiang and H. T. Hou, Simulation of longitudinal beam dynamics with the third harmonic cavity for SSRF phase II project, in *Proceedings of 12th Symposium on Accelerator Physics, SAP2014, Lanzhou, China* (JACoW, Lanzhou, China, 2014), THPMH4, pp. 118–120, https://accelconf.web.cern.ch/SAP2014/papers/thpmh4.pdf.

[25] T. L. He, W. W. Li, Z. H. Bai, and L. Wang, Longitudinal equilibrium density distribution of arbitrary filled bunches in presence of a passive harmonic cavity and the short range wakefield, Phys. Rev. Accel. Beams **24**, 044401 (2021).